

# Mechanical Properties, Flame Retardancy, Hot-Air Ageing, and Hot-Oil Ageing Resistance of Ethylene-Vinyl Acetate Rubber/Hydrogenated Nitrile-Butadiene Rubber/Magnesium Hydroxide Composites

Shuguo Chen,<sup>1</sup> Yong Zhang,<sup>1</sup> Ruyin Wang,<sup>1</sup> Haiyang Yu,<sup>1</sup> Martin Hoch,<sup>2</sup> Sharon Guo<sup>2</sup>

<sup>1</sup>State Key Laboratory of Metal Matrix Composites, School of Chemistry and Chemical Technology, Shanghai Jiao Tong University, Shanghai 200240, China

<sup>2</sup>LANXESS Chemical (Shanghai) Co., Shanghai 200040, China

Received 15 December 2008; accepted 10 April 2009

DOI 10.1002/app.30620

Published online 7 August 2009 in Wiley InterScience (www.interscience.wiley.com).

**ABSTRACT:** The mechanical properties, flame retardancy, hot-air ageing, and hot-oil ageing resistance of ethylene-vinyl acetate rubber (EVM)/hydrogenated nitrile-butadiene rubber (HNBR)/magnesium hydroxide (MH) composites were studied. With increasing HNBR fraction, elongation at break and tear strength of the EVM/HNBR/MH composites increased, whereas the limited oxygen index and Shore A hardness decreased slightly. Hot-air ageing resistance and hot-oil ageing resistance of the composites became better with increasing HNBR fraction. Thermal gravimetric analysis results demonstrated that the presence of MH and low HNBR fraction could improve the thermal stability of the composites. Differential scanning calorimeter revealed that the glass transition temperature ( $T_g$ ) of the composites shifted toward low

temperatures with increasing HNBR fraction, which was also confirmed by dynamic mechanical thermal analysis. Atomic force microscope images showed MH has a small particle size and good dispersion in the composites with high HNBR fraction. The flame retardancy, extremely good hot-oil ageing, and hot-air ageing resistance combined with good mechanical properties performance in a wide temperature range ( $-30^{\circ}\text{C}$  to  $150^{\circ}\text{C}$ ) make the EVM/HNBR/MH composites ideal for cables application. © 2009 Wiley Periodicals, Inc. *J Appl Polym Sci* 114: 3310–3318, 2009

**Key words:** hydrogenated nitrile butadiene rubber; ethylene vinyl acetate rubber; mechanical properties; flame retardancy; hot-air ageing and hot-oil ageing resistance; composite

## INTRODUCTION

In recent years, the production of elastomeric blends has markedly increased, due to their well balanced physical and mechanical properties, easy processability and relatively low cost. Blending of two or more types of polymers is a very useful technique for the preparation and development of materials with properties superior to those of the individual constituents. Ethylene-vinyl acetate rubber (EVM) with different high vinyl acetate (VA) content is extensively used in many fields, such as in cables industry.<sup>1–3</sup> In cables application, flame retardants should be introduced into EVM to reduce flammability. Aluminum hydroxide and magnesium hydroxide (MH) are typical flame retardants, but usually high filler content is required to obtain satisfying flame retardancy.<sup>4,5</sup>

However, the high content of superfluous MH usually leads to poor low-temperature bending property<sup>6</sup> and decreasing mechanical performance for EVM composites,<sup>7</sup> such as tear strength, elongation at break. It is necessary to improve mechanical properties of EVM composites while maintaining its flame retardancy. EVM also has a relatively poor hot-oil ageing and hot-air ageing resistance in comparison with fluororubber or hydrogenated nitrile-butadiene rubber (HNBR), which should be considered in special cables industry.<sup>8–10</sup> HNBR provides excellent mechanical properties<sup>11–13</sup> (such as high tensile strength, excellent cold bending property, and abrasion resistance, etc.), as well as hot-oil ageing and hot-air ageing resistance, has been widely used in industry. Generally, HNBR is immiscible with most commercial elastomers. It is, however, miscible with certain chlorinated polyethylenes and poly(vinyl chloride). In this work, EVM and HNBR were mixed with high MH content to obtain competitive properties and their mechanical properties, flame retardancy, hot-air ageing, and hot-oil ageing resistance were investigated.

Correspondence to: Y. Zhang (yong\_zhang@sjtu.edu.cn).

## EXPERIMENTAL

### Materials

EVM with 70 wt % of VA (UML1+4, 100°C, 68) and HNBR with 39 wt % acrylonitrile (ACN) (UML1+4, 100°C, 70) were provided by LANXESS Chemical Co. (Shanghai, China). Unmodified lamellar crystal nano-MH with an average length of 90 nm and thickness of 20 nm was made by Shanghai Allrun High-Tech Co. (Shanghai, China) Vinyltrimethoxysilane (A171) was supplied by Shanghai Huarun Chemical Group Co. (Shanghai, China) Zinc borate, tricresyl phosphate (TCP), vulkanox DDA, aflux 18, antilux 654, and triallyl isocyanurate were provided by Rhein Chemi. Co. (Shanghai, China) Dicumyl peroxide (DCP) with 97% purity was supplied by Shanghai Gaoqiao Petroleum Co., China.

### Preparation

All samples were prepared on an open two-roll mill of laboratory size (S(X)K-160A, size: 320 × 160 mm, Shanghai Rubber Machinery Factory, China) at room temperature through following procedures: EVM and HNBR with different weight ratio (EVM/HNBR = 100/0, 90/10, 75/25, 50/50, 25/75, 0/100) were first mixed with auxiliary materials. Then MH (150 phr, phr = parts per hundreds part of rubber) with TCP and A171 was added. DCP (3 phr) was added in the end. The composites were sheeted out 10 times on a two-roll mill to form 3- to 5-mm thick. The obtained composites were finally compressed curing at 170°C for 15 min under 10 MPa into sheets of suitable thickness. All samples were preconditioned at 23°C for 24 h before tested.

### Measurement and characterization

#### Flame retardancy

The limited oxygen index (LOI) was measured according to ASTM D2863 with specimen dimension 130 × 6.5 × 3 mm<sup>3</sup> using an LOI tester (Rheometric Scientific Ltd., USA). Vertical burning test was carried out with specimen dimension of 130 × 13 × 3 mm<sup>3</sup> according to UL-94 by using a vertical burning test instrument.

#### Mechanical properties

The tensile strength was measured with dumbbell specimens according to ASTM D412-97, using a universal electromechanical tester (Instron series IX.4465, USA) with a crosshead speed of 500 mm/min. Unnotched 90° angle and trousers tear test were tested according to ASTM D624-98, using a universal electromechanical tester (Instron series

IX.4465) with a crosshead speed of 500 mm/min and 50 mm/min, respectively. Shore A hardness was measured according to ASTM D2240-97 using a hand-held Shore A durometer.

#### Hot-oil ageing and hot-air ageing resistance

The hot-oil ageing resistance was evaluated according to ASTM D471-98. The samples were immersed in IRM 903 oil at 100°C for 24 h. The hot-air ageing resistance was tested according to ASTM D573-99. The samples were placed in a hot-air oven at 150°C for 7 days.

#### Thermal gravimetric analysis (TGA)

The thermal degradation behaviors of the composites were studied by a thermal gravimetric analyzer (TGA, TGA7, Perkin Elmer) at a heating rate of 10°C/min (from 20°C to 800°C) under nitrogen.

#### Differential scanning calorimeter analysis (DSC)

The glass transition temperatures ( $T_g$ ) of the composites were measured by a differential scanning calorimeter (DSC, Pyris 1, Perkin Elmer) at a heating rate of 20°C/min (from -60°C to 40°C). Before tested, the samples were cooled to -60°C at a cooling rate of 10°C/min.

#### Dynamic mechanical thermal analysis (DMTA)

The dynamic mechanical properties of the composites were measured by a dynamic mechanical thermal analyzer (DMTA, IDMA2980, TA) at a heating rate of 3°C/min (from -80°C to 70°C) and a frequency of 1 Hz with 0.01% strain. Before tested, the samples are cooled to -80°C at a cooling rate of 10°C/min.

#### Morphology

The morphologies of the composites were observed by a bioscope atomic force microscopy (AFM) (Bioscope, Veeco Instruments).

## RESULTS AND DISCUSSION

### Flame retardancy

Figure 1 shows with increasing HNBR fraction, the LOI of the composite decreases gradually, but is still over 30, suggesting the composites have excellent flame retardancy. The decrease of LOI is due to the poor flame retardancy of HNBR.<sup>14</sup> All EVM/HNBR/MH composites can survive in the UL-94 vertical burning test with V-0 level. No dripping was observed for all samples in both two times of

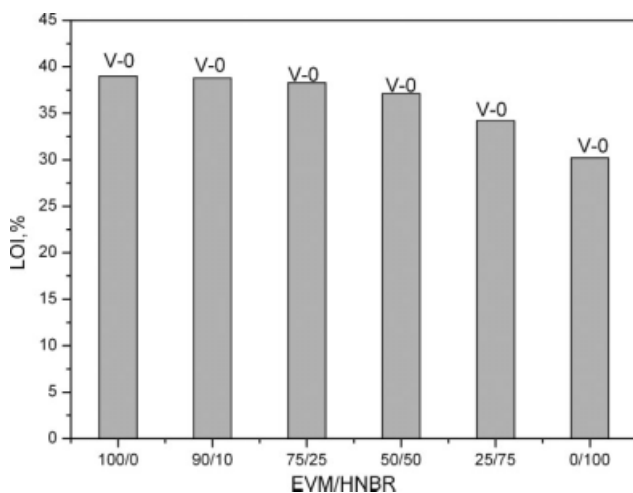


**Figure 1** LOI and UL-94 of EVM/HNBR/MH composites.

ignition, suggesting MH has good flame retardancy for EVM/HNBR composites. The combination of MH fillers was present in all compounds and could have contributed the good mechanical properties as well as to the good LOI values.<sup>15,16</sup> All samples have an excellent self-extinguishing property after ignition and could meet the demands for cables application<sup>2,6</sup> as the concentration of the combustible organic constituents is reduced by adding MH. In addition, MH eliminates water, thus withdrawing energy, from the flames, thus reduces the flammability of combustible polymers.<sup>17,18</sup>

### Mechanical properties

The mechanical properties of EVM/HNBR/MH composites are shown in Figure 2. The elongation at break, angle tear strength, and trousers tear strength increase with increasing HNBR fraction. The elongation at break, angle tear strength, and trousers tear strength increase from 223%, 40.7 N/mm, 8.9 N/mm for EVM/MH composite to 255%, 44.9 N/mm, 13.0 N/mm for EVM/HNBR/MH (75/25) composite; The shore A hardness and tensile set modulus decrease with increasing HNBR fraction, indicating the crosslinking density decreased in the blends. The low-temperature bending property becomes better when HNBR content is more than 25 phr, indicating HNBR is more feasible than EVM. EVM/HNBR/MH composites have higher elongation at break and tear strength than EVM/MH composite, which can attribute to that HNBR with excellent flexibility is superior to EVM in tensile strength, elongation at break, and tear strength, as well as the good compatibility and heterogeneous covalent crosslinking between EVM and HNBR as both of them are polar rubber.<sup>19</sup> Many papers showed if

two rubbers (such as EPDM/NBR<sup>20</sup> and NBR/SBR<sup>21</sup>) are not compatible, they would show best mechanical properties with a special ratio, due to their relative uniform distribution of components. Although in EVM/HNBR blends, the mechanical properties changed regularly with increasing HNBR fraction, indicating the EVM and HNBR are

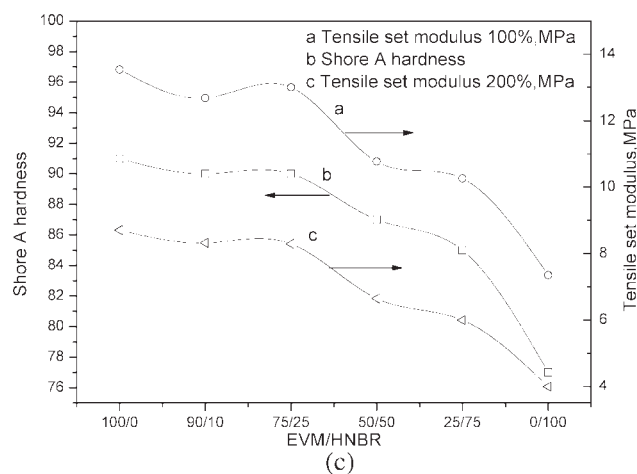
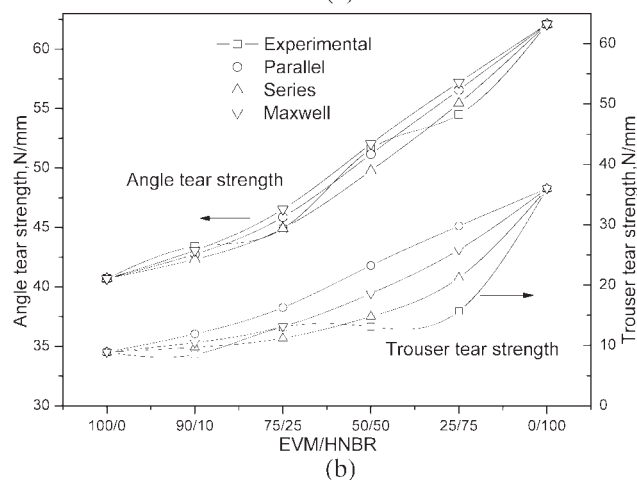
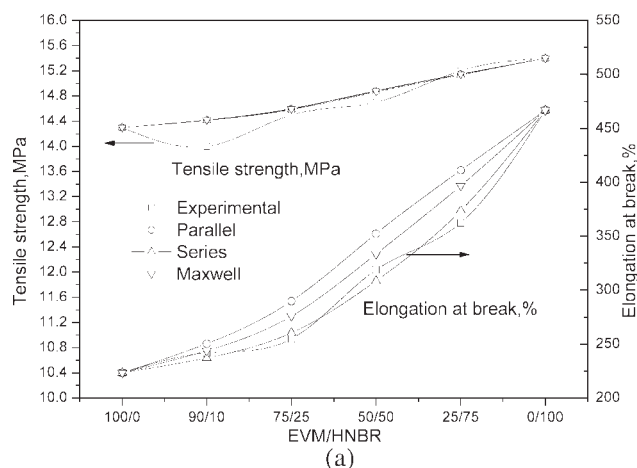


**Figure 2** Mechanical properties of EVM/HNBR/MH composites (a) Tensile strength and elongation at break, (b) 90°-angle tear strength and trousers tear strength, and (c) Shore A hardness and tensile set modulus.

compatible with each other; the flexibility and elasticity of the rubber chains were more when HNBR was incorporated into EVM, which also resulted in less rigid rubber vulcanizates and a decrease in hardness.<sup>22</sup>

Mechanical properties of blends are widely studied through a comparison of experimental results and prediction based on various theoretical models. Different theoretical model selected to predict the mechanical behaviors of EVM/HNBR/MH systems include parallel,<sup>23</sup> series,<sup>23</sup> and Maxwell models.<sup>23</sup>

The parallel model given by following equation is a highest upper bound model.

$$M = M_1\chi_1 + M_2\chi_2 \quad (1)$$

$M_1$  and  $M_2$  are the mechanical properties, and  $\chi_1$  and  $\chi_2$  are the volume fraction of the components EVM and HNBR, respectively. In this model, the components are considered to be arranged parallel to one another, so that the applied stress elongates each of the components by the same amount.

The series model given the following equation is the lowest lower bound model.

$$1/M = \chi_1/M_1 + \chi_2/M_2 \quad (2)$$

As per Maxwell model

$$M = M_1[M_2 + 2M_1 - 2\chi_2(M_1 - M_2)]/[M_2 + 2M_1 + \chi_2(M_1 - M_2)]$$

The comparison between experimental and three theoretical curves of the tensile strength, elongation at break, and tear strength are also showed in Figure 2. All the three models show almost same positive trend for each and every composite, especially the result of series model is coincided with experimental result, which also indicating the EVM and HNBR are compatible with each other.

#### Hot-oil ageing and hot-air ageing resistance test

Hot-oil ageing resistance is closely related to the polarity of an elastomer. The polarity of EVM is determined by VA content and the polarity of HNBR elastomer is determined by acrylonitrile content.<sup>24</sup> The hot-oil ageing resistance and hot-air ageing resistance of EVM/HNBR composites are summarized in Figure 3. After hot-air ageing (at 150°C in hot-air for 7 days), the tensile strength of all samples increased, which can be due to good thermal stability of C—C crosslinking in peroxide cured system; hot-air ageing is available to formation of additional crosslinking due to high temperature and thus enhanced tensile strength.<sup>25</sup> The tensile strength increases with increasing HNBR fraction as HNBR has a more excellent hot-air ageing resistance, which

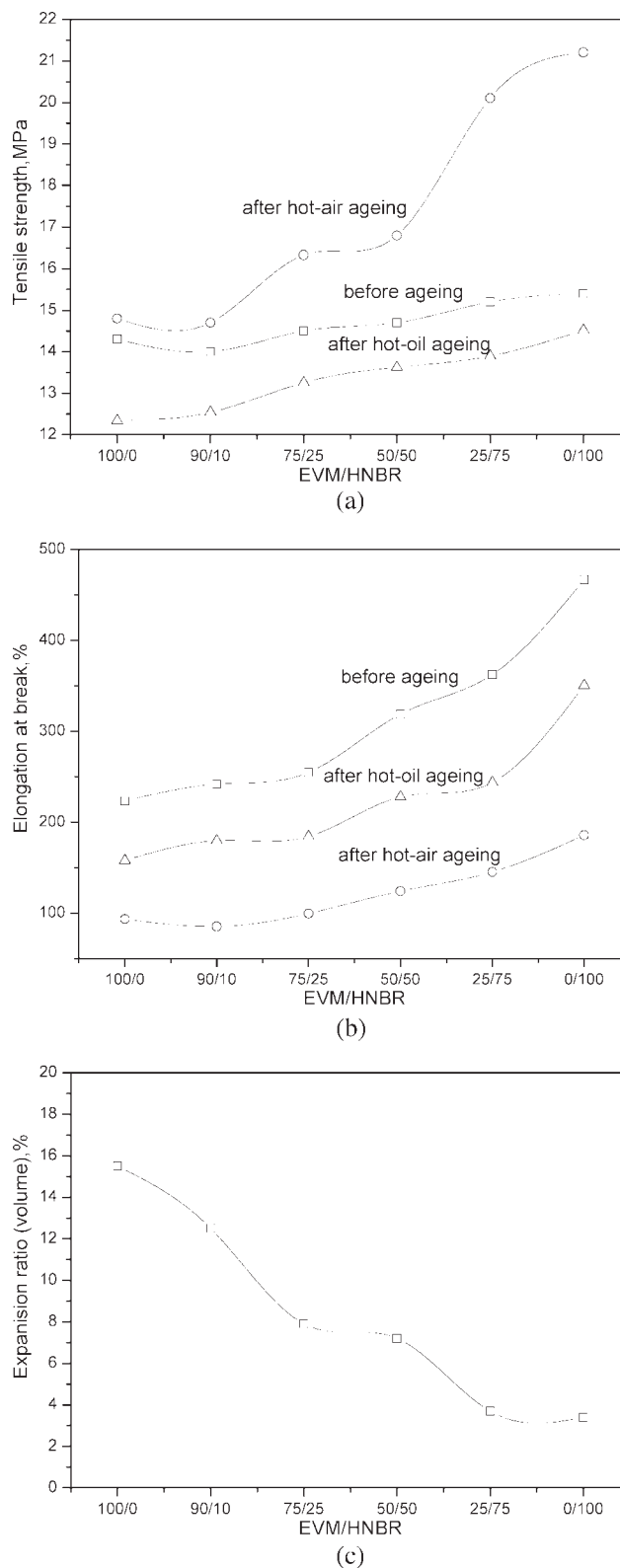


**Figure 3** Hot-oil ageing and hot-air ageing resistance of EVM/HNBR/MH composites (a) tensile strength, (b) elongation at break, and (c) swelling ration (volume) in hot-oil ageing.

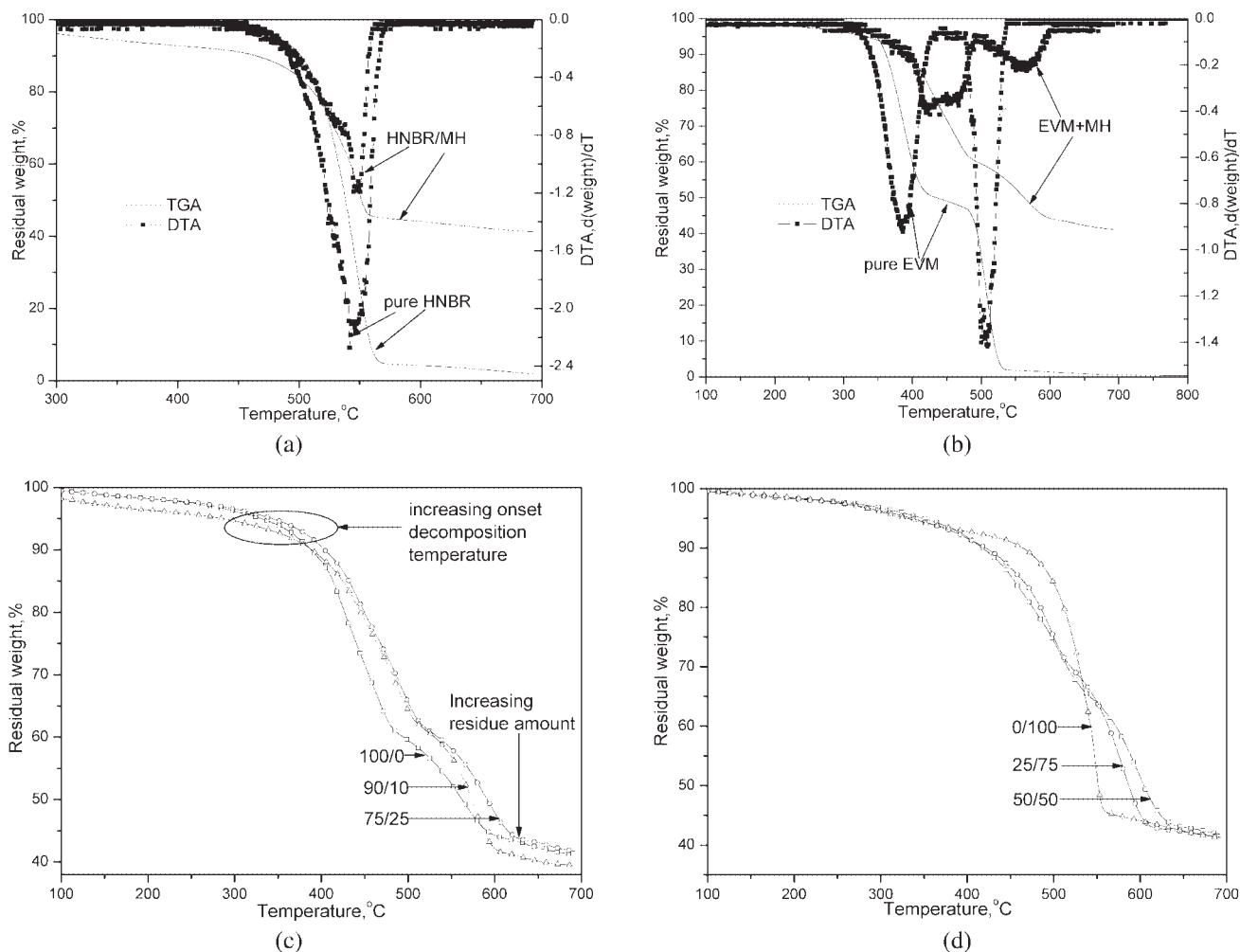


**Figure 4** TGA curves of EVM/HNBR/MH composites (a) TGA curves of HNBR and HNBR/MH composites, (b) TGA curves of EVM and EVM/MH composites, (c) TGA curves of EVM/HNBR/MH with low HNBR fraction, and (d) TGA curves of EVM/HNBR/MH with high HNBR fraction.

can be due to its higher crosslinking density than EVM.<sup>11</sup> However, the overall decrease of elongation at break of  $\sim 60\%$  for aged samples is surprising. This can be due to the formation of additional crosslink as a kind of postcure and a change toward a tighter filler network after tempering, as there is an additional interaction of MH filler to create a stiffer and stronger network with shorter elongation at break after hot-air ageing.<sup>24</sup>

In the hot-oil ageing resistance test, the tensile strength and elongation at break of all samples decrease after hot-oil ageing (at  $100^\circ\text{C}$  in oil for 24 h). With increasing HNBR fraction, the tensile strength increases and volume swelling ratio decreases. The hot-oil ageing resistance of composites could be attributed to the high polarity generated by a high VA content (70%) in EVM whereas in HNBR, the polarity is inherent the high dipole-dipole effect of the ACN group, which presents large electron affinity, allowing the forma-

tion of cyclic structure together with  $>\text{CH}-$  groups that result in intermolecular and intramolecular bridging of macromolecular free radicals.<sup>26</sup> HNBR has a better hot-oil ageing resistance than EVM as HNBR has a stronger polar group than EVM.<sup>12</sup>

## Thermal analysis

### TGA

TGA curves of composites are shown in the Figure 4. The degradation of EVM starts at  $310^\circ\text{C}$  and completes at  $540^\circ\text{C}$ , undergoes two degradation steps.<sup>27</sup> The first decomposition step is due to the loss of acetic acid at the range of  $350^\circ\text{C}$ – $450^\circ\text{C}$  by chain stripping and it leads to the formation of poly(ethylene-co-acetylene), which degrades in the second step.<sup>4</sup> The second degradation step in the range of  $450^\circ\text{C}$ – $550^\circ\text{C}$  involves random scission of backbone followed by radical transfer to allylic position,<sup>15,17</sup>

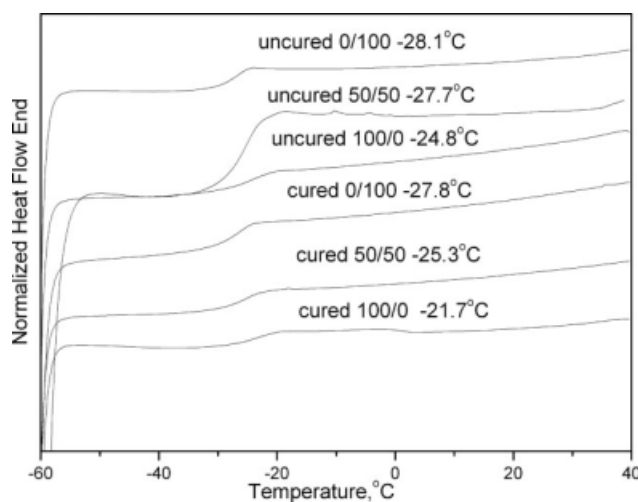


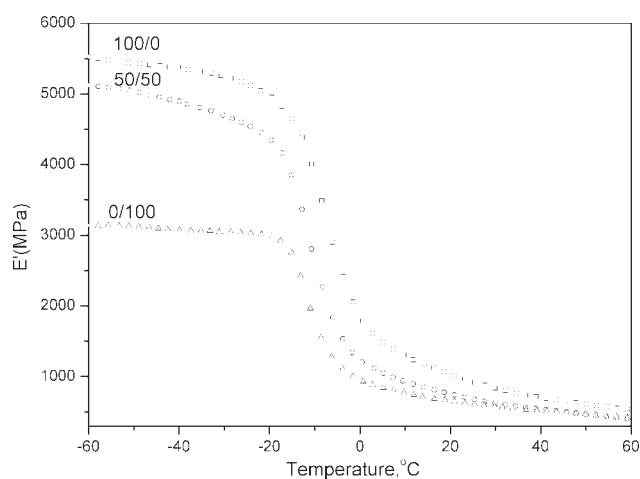
Figure 5 DSC curves of EVM/HNBR/MH composites.

therefore, either hydrogen loss or abstraction can lead to formation of either an unsaturated or saturated chain end, respectively.<sup>4</sup> Depending on what happens on the other end of the radical, the degradation products could be alkanes, terminal alkenes, or dienes.<sup>28</sup> The degradation of HNBR only has a stage which starts at 450°C and completes at 550°C. Hence, HNBR is stable up to 450°C, which is higher than EVM. The degradation of MH starts at 350°C and ends at 400°C, which is corresponding to the dehydration of MH and formation of magnesia.

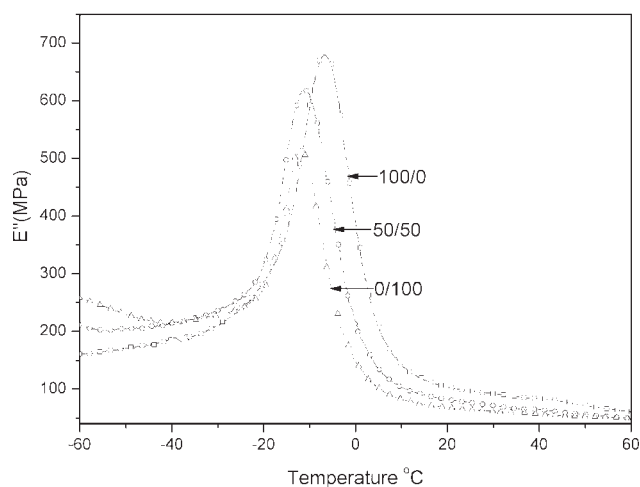
In the EVM/MH composite or HNBR/MH composite, the incorporation of MH improves the thermal stability of EVM or HNBR [Fig. 4(a,b)]. In the EVM/MH composite, the temperature range of first step is extended from 350°C to 480°C and the second step is prolonged from 450°C to 600°C, besides, the stage of degradation of EVM/MH or HNBR/MH is not distinct and the curves become smooth. The incorporation of MH lowers the decomposition rate of the second step but accelerates the loss of acetic acid.<sup>29</sup> The hydroxyl group on MH can assist  $\beta$ -hydrogen leaving,<sup>1</sup> which means the loss of acetic acid can be catalyzed by MH. The residue may contain some carbonaceous materials, which means that the residue obtained from EVM/HNBR/MH nanocomposites not only contains metal oxide but also has some carbonaceous material.

Figure 4 (c,d) shows the TGA curves of EVM/HNBR/MH composites. The incorporation of HNBR increases the initial degradation temperature of EVM/HNBR/MH, which may be due to the stable cyclization on nitrile structures.<sup>26</sup> With increasing HNBR fraction, the degradation of the composites corresponding to the first and second degradation steps occurred at a higher temperature [Fig. 4(c)]. The EVM/HNBR/MH (90/10) has a higher terminal

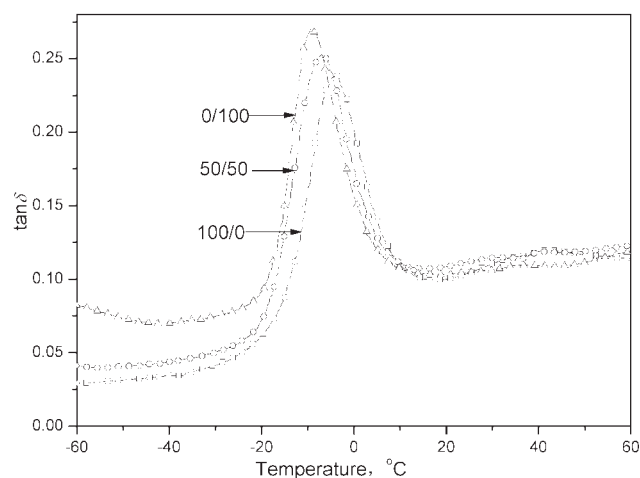
degradation temperature) (520°C) of first stage than that of EVM/MH composite (480°C), whereas the first stage degradation curve of EVM/HNBR/MH



(a)



(b)



(c)

Figure 6 DMTA curves of EVM/HNBR/MH composites (a) storage modulus, (b) loss modulus, and (c) loss factor.

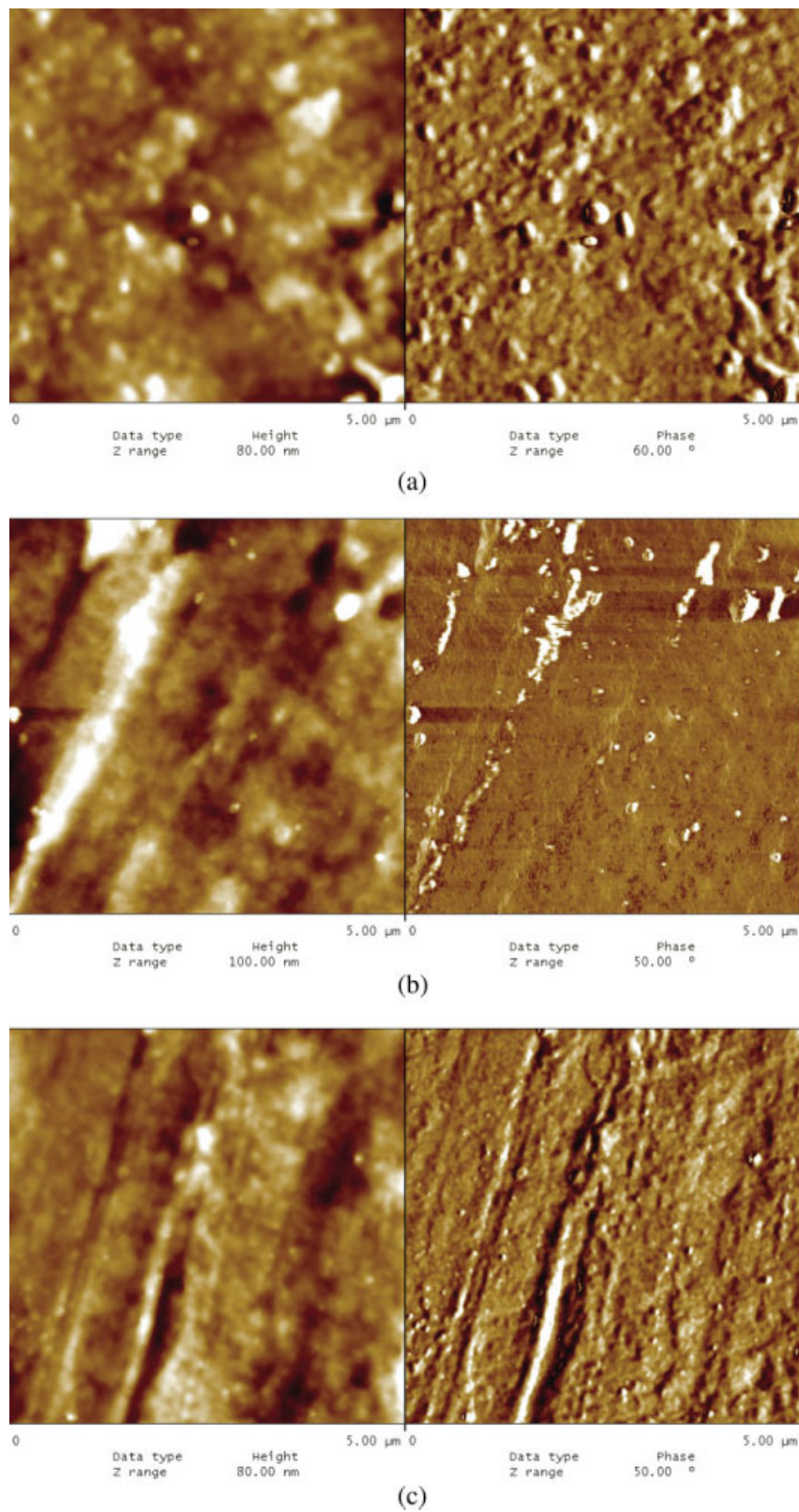


**Figure 7** AFM images of EVM/HNBR/MH composites (a) EVM/MH, (b) EVM/HNBR/MH (50/50), and (c) HNBR/MH. [Color figure can be viewed in the online issue, which is available at [www.interscience.wiley.com](http://www.interscience.wiley.com).]

(75/25) nearly overlaps with that of EVM/HNBR/MH (90/10), but the terminal degradation temperature of second stage increases. It means low HNBR

content in the EVM/HNBR/MH composites would increase the thermal decomposition temperature. It is interesting to note that at high HNBR fraction, the

TGA curve of EVM/HNBR/MH (25/75) in the first stage is nearly same with that of EVM/HNBR/MH (50/50). It indicates a large amount of HNBR could not increase the terminal temperature of EVM/HNBR/MH in the first degradation stage.

### DSC

To investigate the compatibility of EVM/HNBR blends, DSC analysis was performed to measure glass transition temperature ( $T_g$ , onset) as a function of composition. The DSC curves of EVM/HNBR/MH composites show that each sample has only one  $T_g$ , which may indicate that the EVM and HNBR are compatible.<sup>30</sup> The two separate  $T_g$  platforms merged into a single-broad platform spanning a temperature range larger than the characteristic  $T_g$  values of the individual phases. As showed in Figure 5, the  $T_g$  of EVM/HNBR/MH composites shift to lower temperature with increasing HNBR fraction, as HNBR has a lower  $T_g$  than EVM. After vulcanization, the  $T_g$  moves to higher temperature zone. It is due to the crosslinking effect of DCP. The mobility of polymer segments in a wide-operating temperature range reduces the crystallization risk and the hardening effect on the polymer. This can be expected in fixed cables for platform located in regions with harsh environments.<sup>14</sup>

### DMTA

The temperature dependence of loss modulus ( $E''$ ), storage modulus ( $E'$ ), and loss factor ( $\tan \delta$ ) is showed in Figure 6. As expected there is appearance of one  $T_g$  corresponding to homogeneity of the blend components as observed from Figure 6(c). It has been reported that molecular level mixing is more homogeneous when  $T_g$  corresponding to individual rubber are closer is well documented.<sup>31</sup> The EVM and HNBR have the similar polar and their  $T_g$  are closer, which can be concluded that EVM and HNBR are mixed on molecular level.

The  $E'$  and  $E''$  of EVM/MH composite are higher than that of HNBR/MH composite. It seems that the  $E'$  and  $E''$  decrease with increasing HNBR fraction. Increasing HNBR fraction leads to an enhancement of  $\tan \delta_{\max}$ . The  $T_g$  values decrease with increasing HNBR fraction. The  $T_g$  (DMTA) values of EVM/MH, EVM/HNBR/MH (50/50) and HNBR/MH composites were  $-4.4^\circ\text{C}$ ,  $-7.1^\circ\text{C}$ , and  $-9.5^\circ\text{C}$ , respectively, which is also due to the feasible of HNBR.

### Morphology

The AFM micrographs of the EVM/HNBR/MH composites are shown in Figure 7. In Figure 7(a), MH has some aggregation as there are some large

bright domains, whereas in Figure 7(c), MH particles are dispersed well in the polymer matrix and the aggregation is not clear, showing an even distribution of broader features at the interface, which may be a decrease in surface density due to the incorporation of HNBR.<sup>32</sup> HNBR/MH composite shows smooth surface compared with EVM/MH composite, indicating HNBR has a better dispersion of MH particles than EVM. The image of Figure 7(c) shows discrete particles embedded in the HNBR matrix, which means MH has a better interfacial interaction with HNBR than with EVM. Diameters of discrete MH particles become smaller with increasing HNBR fraction. There is no obvious interface between EVM and HNBR observed in Figure 7(b), which indicates EVM and HNBR are homogeneous covulcanized and compatible.

### CONCLUSIONS

EVM/HNBR/MH composites were prepared by mechanical blending and characterized by DSC, TGA, DMTA, and AFM. Their mechanical properties, flame retardancy, hot-air ageing, and hot-oil ageing resistance were studied. The tear strength and elongation at break of composites increased with increasing HNBR fraction. The composites had good flame retardancy with LOI over 30 and a V-0 level in the UL-94 test. The hot-oil ageing resistance of composites became better with increasing HNBR fraction. TGA revealed that a small content of HNBR could raise the thermal degradation temperatures of EVM/MH composites. The DSC and DMTA data indicated that HNBR could decrease the  $T_g$  values and improve the flexibility of composites; EVM and HNBR are homogeneous covulcanized and compatible. The storage modulus, loss modulus, and  $\tan \delta$  of the composites decreased with increasing HNBR fraction. MH had small particle size and good dispersion for the composites with high HNBR fraction.

### References

1. Beyer, G. *Fire Mater* 2001, 25, 193.
2. Riva, A.; Camino, G.; Fomperie, L. *Polym Degrad Stab* 2003, 82, 341.
3. Zilberman, J.; Hull, T.; Price, D. *Fire Mater* 2000, 24, 159.
4. Camino, G.; Maffezzoli, A.; Braglia, M.; Zapparano, M. *Polym Degrad Stab* 2001, 74, 457.
5. Pradeep, M. A.; Vasudev, N.; Reddy, P. V.; Khastgir, D. *J Appl Polym Sci* 2007, 104, 3505.
6. Huang, H.; Tian, M.; Liu, L.; Liang, W.; Zhang, L. *J Appl Polym Sci* 2006, 100, 4461.
7. Huang, H.; Tian, M.; Liu, L. *J Appl Polym Sci* 2008, 107, 3325.
8. Çopuroglu, M.; Sen, M. *Polym Adv Technol* 2004, 15, 393.
9. Radhakrishnan, C. K.; Alex, R.; Unnikrishnan, G. *Polym Degrad Stab* 2006, 91, 902.



10. Sen, M.; Copuroglu, M. *J Therm Anal Calorim* 2006, 86, 223.
11. Geralda, S.; White, J. L. *J Appl Polym Sci* 2000, 78, 1524.
12. Geralda, S.; White, J. L. *J Appl Polym Sci* 2005, 95, 2.
13. Zhao, W. *J Appl Polym Sci* 1994, 54, 1199.
14. Meisenheimer, H. *Rubber World* 1991, 204, 19.
15. Fernandez, A. I.; Haurie, L.; Formosa, J.; Chimenos, J. M.; Antunes, M.; Velasco, J. I. *Polymer Degrad Stab* 2008, 94, 57.
16. Wang, Z.; Qu, B.; Fan, W.; Huang, P. *J Appl Polym Sci* 2001, 81, 206.
17. Carpentier, F.; Bourbigot, S.; Le Bras, M.; Delobel, R.; Foulon, M. *Polym Degrad Stab* 2000, 69, 83.
18. Fu, M.; Qu, B. *Polym Degrad Stab* 2004, 85, 633.
19. Yang, Q. *Modern Rubber Technology*; Sinopec Press: Beijing, 2007.
20. Manoj, K. C. *J Appl Polym Sci* 2007, 105, 908.
21. Habeeb Rahiman, K.; Unnikrishnan, G.; Sujith, A.; Radhakrishnan, C. K. *Mater Lett* 2005, 59, 633.
22. Vinod, V. S.; Varghese, S.; Alex, R.; Kuriakose, B. *Rubber Chem Technol* 2001, 74, 236.
23. Thomas, S.; George, A. *Eur Polym J* 1992, 28, 1451.
24. He, M. *Polymer Physics*; Fudan University Press: Shanghai, 2005.
25. Brown, R. *Physical Testing of Rubbers*, 3rd ed.; Chapman and Hall: London, 1996.
26. Giurginca, M.; Zaharescu, T. *Polym Bull* 2003, 49, 357.
27. Basfar, A.; Ccaron, J. M.; Shukri, T. M.; Bahattab, M. A.; Courdreuse, P. N. A. *J Appl Polym Sci* 2008, 107, 642.
28. Costache, M. C.; Jiang, D. D.; Wilkie, C. A. *Polymer* 2005, 46, 6947.
29. Gui, H.; Zhang, X.; Dong, W.; Wang, Q.; Gao, J.; Song, Z.; Lai, J.; Liu, Y.; Huang, F. *Polymer* 2007, 48, 2537.
30. Varghese, H.; Bhagawan, S. S.; Rao, S. S. *Eur Polym J* 1995, 31, 957.
31. Magaraphan, R.; Thajaroen, W.; Lim-Ochakun, R. *Rubber Chem Technol* 2003, 76, 406.
32. Yuan, X.; Zhang, Y.; Peng, Z. *J Appl Polym Sci* 2002, 84, 1403.